High Speed Asynchronous Motor with High T_c Superconducting Bearings

C. DELPRETE,* G. GENTA,* L. MAZZOCCHETTI,** E. RAVA,** A. RICCA,***
G. RIPAMONTI,*** L. SANTINI,* A. TONOLI,* E. VARESI*** AND S. ZANNELLA***

ABSTRACT

The discovery of High T_c Superconductors has renewed the interest for practical applications of superconductivity including devices based on magnetic levitation. To evaluate their potential use for near-frictionless high speed passive magnetic bearings, a prototype of an asynchronous motor with the rotor floating on two melt textured $YBa_2 Cu_3 O_{7-x}$ suitably shaped blocks has been built and tested.
The low radial stiffness of the bearings compels one to use non-conventional motor configurations, in order to avoid radial instability under load. In the present paper the design of the electric motor and the experimental testing of the superconducting bearings, in terms of levitation force versus rotor height and magnetic stiffness, are described. The characterization of the bearings allows one to perform a rotor-dynamics study of the whole machine, whose results are then validated experimentally. The bearing drag is evaluated through spin-down tests.

INTRODUCTION

Since the discovery of high T_c superconductors (HTS) a considerable research activity has been devoted to this field because of their potential for technological advancement [1]. A serious hindrance to the development of high current applications, based on high T_c wires, as power transmission and high field magnets, is their low current-carrying capacity at 77 K caused mainly by grain boundary weak links and inadequate flux pinning energy. A remarkable progress for eliminating these problems in the $YBa_2Cu_3O_{7-x}$ (usually referred to as Y-123) superconductor has been reached by melt-texturing-type processing [2].
However it is difficult to apply these techniques in the fabrication of long wires while they are successful for the preparation of monolithic samples whose present properties are good enough for use in superconducting magnetic bearings to be used in high speed rotating machinery, flywheels, gyroscopes, etc. It is believed that magnetic bearings will be one of the nearest-term application of bulk high Tc superconductors (from [3] to [11]).
Superconducting magnetic suspension systems based on Meissner-Ochsenfeld effect, i.e. on the tendency of superconducting materials to expel the magnetic flux when cooled below the critical temperature T_c, were considered even before the discovery of high T_c superconductors [12], but became an attractive solution only after material with high critical temperature (slightly above the boiling temperature of liquid nitrogen at standard pressure) were produced.
A first advantage of diamagnetic suspension systems is their inherent stability, which allows one to build a passive suspension on five axes: actually the limitation in stability stated by Earnshaw's theorem does not hold in the case of diamagnetic suspensions [12]. Another advantage is their very low drag, which can be evaluated as about 1000 times less than that of rolling elements

* Dipartimento di Meccanica, Politecnico di Torino, C.so Duca degli Abruzzi 24, 10129 Torino, Italy
** Elettrorava S.p.A., v. Don Sapino 176, 10040 Savonera, Torino, Italy
*** CISE S.p.A., P.O. Box 12081, 20134 Milano, Italy.

bearings and 25 times less than that of the best existing conventional magnetic bearing systems. The obvious disadvantages of producing low levitation forces and of needing low temperature cooling (with present materials at about the boiling temperature of liquid nitrogen) seem to be potentially reduced with the progress in the field of superconductor materials.
Meissner- Ochsenfeld effect is a fundamental aspect of superconductivity, in addition to the zero resistivity, leading to a repulsive force between superconductors and permanent magnets which can be used to perform magnetic levitation. For type II superconductors, complete flux expulsion takes place only at very low fields, below the first critical field H_{c1}, while at higher values the magnetic flux generated by the permanent magnet starts to penetrate within the superconductor in form of vortices which are pinned by inhomogeneities and defects of the material. The repulsive force due to the Meissner effect is small while higher values can be reached when the superconductor exhibits flux pinning.
In the latter case the force-distance characteristic for the repulsive force between the superconductor and the magnet exhibits a hysteretic nature [8] and several stable equilibrium positions of the levitating magnet can be observed. In the case of a cylindrical permanent magnet levitating with its axis parallel to the HTS surface, any translational motion in a direction parallel or perpendicular to the surface causes a reaction which has a "restoring force" and a "damping force" component, as expected owing to the hysteretic behaviour of the material, while the rotational symmetry of the magnetic field allows a nearly frictionless spinning of the permanent magnet itself. The magnetic drag torque, giving rise to energy dissipation, is very low (values of the order of 10^{-9} Nm for melt-textured Y-123 have been measured) and it is essentially due to inhomogeneities of the magnetic field of the permanent magnet.
According to the Bean critical state model [13], the levitation force is a function of the external field and is proportional to the critical current density J_c and to the diameter d of the shielding current loops, thus depending strongly on the HTS microstructure. The best results are obtainable with melt processed $YBa_2Cu_3O_{7-x}$ materials characterized by higher magnetization values with respect to sintered samples owing to the improved orientation and connectivity of the superconducting grains and to strong pinning centres whose nature is still questionable. Residual magnetization of about 1.5 T at 77 K and levitation pressures of the order of 10^5 Pa are now achievable, making passive bearings one of the first bulk applications of HTS. Significantly higher trapped field and levitation pressures are obtainable at lower temperatures. The mentioned values can be still improved by neutron irradiation that produces a defect structure acting as strong pinning centres.
Some problems are still linked with magnetic flux creep, i.e. with a reduction in time of the magnetic levitation force which has been recorded [2], [11].
A simple high speed electrical machine with superconducting diamagnetic bearings is described in the present paper. An extensive static and dynamic characterization work was performed in order to gain first-hand experience on the behaviour and potentialities of rotor suspension systems of this kind.

DESCRIPTION OF THE ELECTRICAL MACHINE

A picture of the asynchronous electric motor and a schematic drawing of the rotor and the bearings are shown in Figure 1. The tubular shaft carries at its ends two housings for two cylindrical NdFeB axially polarized permanent magnets on each side, 7.8 mm in diameter and 4 mm thick, mounted with their magnetic axis collinear to the rotor axis. The maximum strength field on their surface is 0.32 T. The whole bell-shaped rotor was machined from a single bar of 2014 aluminium alloy, to insure a minimum amount of "rotating damping" to enhance stability in the supercritical range. The low load carrying capacity of the bearings forced to keep the mass of the rotor to a minimum (18.77 g) while their low stiffness compelled to use an unusual configuration of the rotor magnetic circuit to avoid the so-called unbalanced magnetic pull [12], [14]. The laminated core is then not rotating, so that the air gap is kept constant and electromagnetic forces on the rotor do not depend on its position; this results also on a lighter rotor as well. The part of the rotor in which the driving force is originated by the eddy currents has then the shape of a bell.

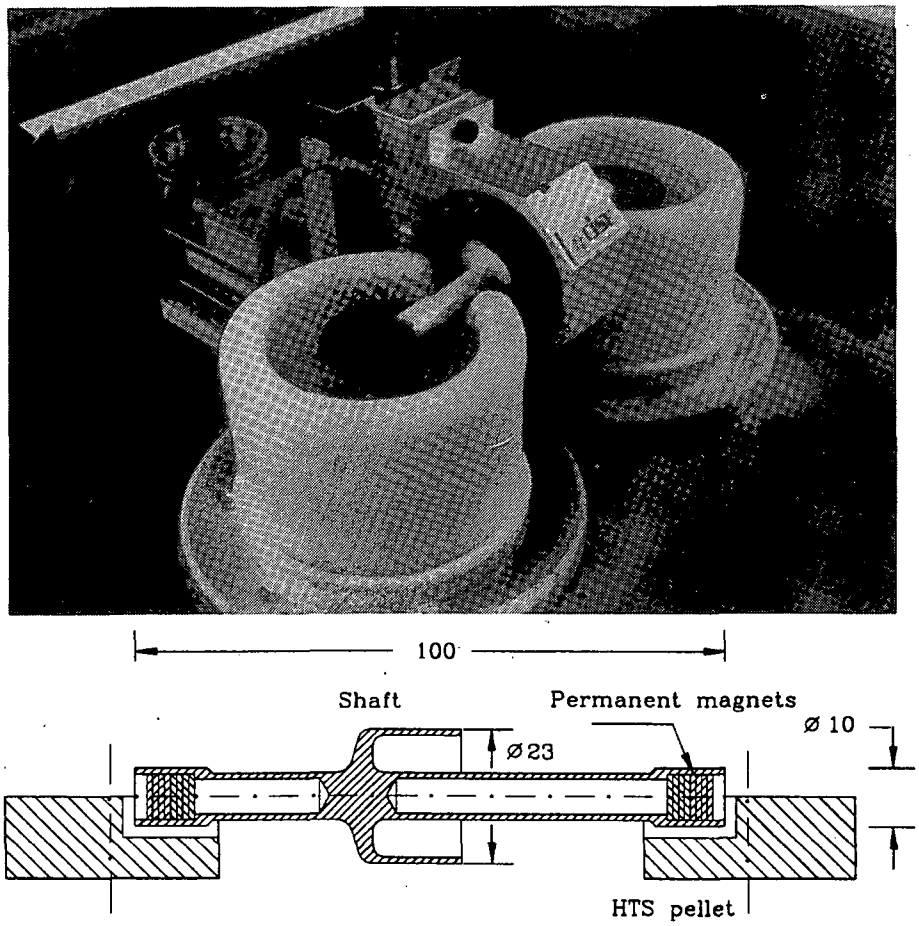

Figure 1. High speed (120000 rpm) asynchronous motor using HTS bearings. Picture and schematic drawing of the rotor and the bearings.

The magnetic bearings are based on a grooved pellet, 36 mm in diameter and 10 mm thick, melt-textured $YBa_2Cu_3O_{7-x}$. This material is of the Y-123 type, made by a modification of the MPMG (Melt Powder Melt Grown) process developed by Murakami [3]. A mixture of $BaCuO_2$ and CuO powders was melted at 1300 °C for a few minutes and then quenched between two copper plates. The quenched product was then ground, mixed with Y_2O_3 powders in the proper stoichiometry, pressed into pellets, heated above the peritectic temperature (1015 °C) where decomposition in a solid Y-211 phase and a liquid phase ($BaCuO_2$, CuO) takes place and slowly cooled to 900 °C to obtain the superconducting Y-123 phase, with a well texturing degree, plus distributed Y-211 particles. The samples were finally oxygenated to optimize their superconducting properties, worked to the final shape which includes a cylindrical slot to increase the lateral magnetic stiffness and coated to prevent degradation due to humidity. The bearings are cooled in glass dewars filled with liquid nitrogen by thermal conduction through oxygen free high conductivity (OFHC) copper blocks.

Three stator coils with a 120° phasing generate the rotating field. The magnetic induction at the air gap is low (0.1 T) in order to ensure low heating due to the relatively high air gap and consequently negligible thermal deformation of the rotor. The electronic drive unit is a three-phase, low voltage frequency converter that automatically controls the rotor up to a speed slightly lower than 120000 rpm, corresponding to a peripheral velocity of 150 m/s.

STATIC CHARACTERIZATION OF THE BEARINGS

Although the displacement velocity is one of the parameters influencing the force-displacement characteristic of the bearing, all tests were conducted in static conditions. In the case of HTS

bearings it is well known that the force is strongly influenced by the relative position between the bearing and the magnet in which the cooling leading to superconducting state is performed and by all the "past history" of the system.
In order to investigate this aspect of the phenomenology of the magnetic force between the HTS bearings and magnetic ends of the rotor several tests were performed cooling the HTS pellets in different positions. After the operating temperature was reached, the magnet was brought at a distance large enough to have negligible magnetic interaction (200 mm; at 50 mm the force was however already too small to be measured). The force was then measured while nearing the magnet up to a fixed distance from the superconducting surface and then while bringing it back. Several cycles were performed and recorded. The temperature was then raised above T_c, a different position of the magnet was reached, superconducting stated was obtained again and the whole measuring procedure was repeated.
The procedure described above was performed for the measurement of the force in direction perpendicular to the surface of the superconducting material (z-direction) using the experimental set-up shown in Figure 2: a model of the shaft extremity is suspended to a load cell whose position is fixed in space. The superconducting bearing, with its dewar container, was secured to a table which had 3 micrometric slides allowing it to be moved in both vertical and horizontal directions. The relative displacement between bearing and shaft was measured through an optical collimator, whose accuracy is of 1 μm. The accuracy of the load cell is of 0.1 mN.
The force F_z measured in vertical direction when the cooling leading to the superconducting state is performed outside the zone of interaction of the magnet (zero-field cooling) is reported in Figure 3a, full lines. The initial characteristic can be accurately approximated as $F = F_o e^{-\alpha z}$ (Figure 3b), with $F_o = 1.31$ N and $\alpha = 307$ m^{-1}. This behaviour is in contrast with the diamagnetic model predicting that the force is inversely proportional to z^4, but has been reported in the literature [4], [5]. When the magnet is moved away from the HTS, the force exhibits a hysteretic behaviour related to the flux pinning occurring for fields higher than H_{c1}. Several hysteresis cycles were recorded, obtaining a very good repeatibility after the second cycle. Owing to hysteresis, different levitation positions are possible between the points A and B in Figure 3a, in which the static repulsive force equals the static load on the bearing. Note that a slight attractive force is displayed when the magnet is moved away from the superconductor owing to the trapped flux. In Figure 3a is also reported the curve obtained by cooling the HTS within the magnetic field, at a distance z=3 mm (dashed line). Note that in this case the force is repulsive when getting nearer to the surface and attractive at higher distance and the slope in the static equilibrium position is higher. The characteristic cooling at z=5mm is reported in Figure 3c, together with a curve obtained with a single magnet. The cooling distance can be chosen as a trade off between the requirements of obtaining a high value of the stiffness "in the small" about the equilibrium position and of insuring a rotor-stator clearance high enough to avoid contacts under the worst running conditions.

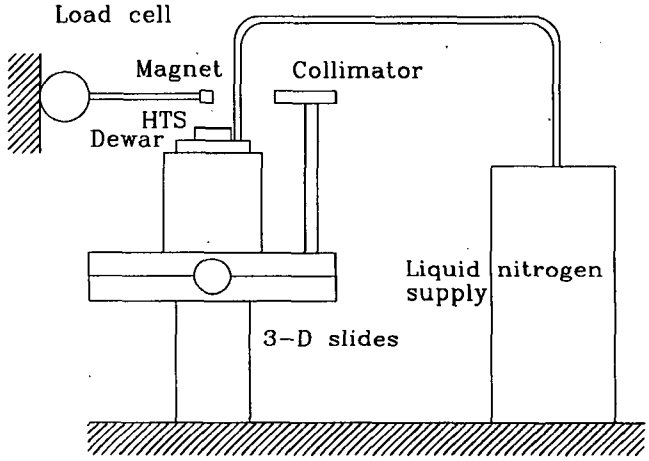

Figure 2. Scheme of the experimental set-up for magnetic force measurements.

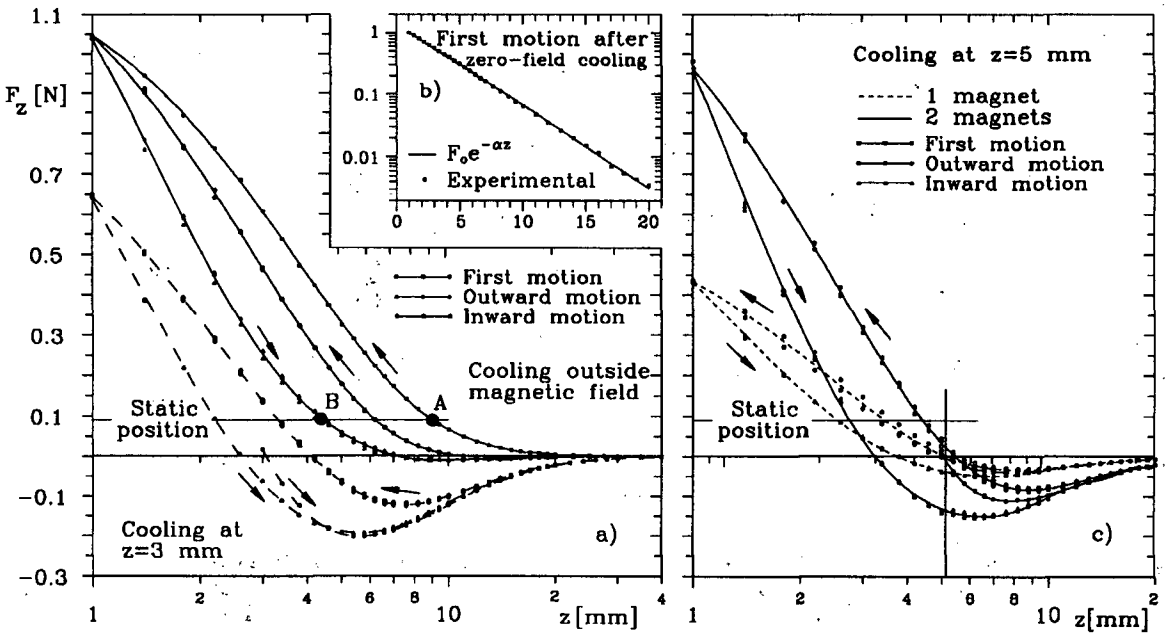

Figure 3. Levitation force as a function of the vertical position of the rotor axis. Different hysteresis cycles related to different cooling positions of the HTS. (a: zero-field cooling and field cooling at z=3 mm; b: first curve for zero-field cooling; c: field cooling at z=5 mm).

The static forces on the two bearings are different (respectively of 0.098 and 0.086 N) as the centre of gravity of the rotor is not at midspan. In the case of cooling at a distance of 5 (3) mm from the surface, the static equilibrium position in which the force is of 0.09 N, is between 2.80 (2.18) and 4.80 (3.33) mm, owing to hysteresis. The levitation force was measured for small displacements about the static equilibrium position, obtaining the hysteresis cycles reported in Figure 4a. The curves were obtained by reaching a position in which the levitation force was of 0.09 N and then cycling about it; after some cycles the form of the curve was stabilized and the cycles were recorded; the central value of the force in cycles so obtained is then slightly different from the value 0.09 N assumed, owing to hysteresis. The behaviour of the bearing can be linearized about the equilibrium position, obtaining a vertical linear stiffness k_z and a relative damping (linear hysteretic damping model) ψ (or a loss factor $\eta = \psi/2\pi$), which can be computed as the ratio of the energy dissipated in a cycle and the potential energy stored between the "central" equilibrium position and the maximum elongation in the cycle. Note that the loss factor obtained in this way must be regarded only as a rough estimate of the damping capabilities of the magnetic suspension. The results are reported in Table I.

The shape of the small hysteresis cycles about the static equilibrium position obtained along an inward branch of a large hysteresis cycle is compared with that obtained along and outward branch in Figure 4b. The plot has been obtained for field-cooling at 5 mm, with large hysteresis cycles of the type shown in Figure 3c. Note that the values of the linearized stiffness are quite different in the two cycles shown.

For the measurement of the force in a direction parallel to the surface (radial (x) and axial (y) directions) a further parameter, namely the distance between the magnet and the surface, must be controlled. All tests in horizontal direction were performed by maintaining the distance between stator and rotor at the nominal value corresponding to a levitation force equal 0.09 N; the results are reported in Figure 5. The lateral and axial stiffness and loss factor for small displacements about the static equilibrium position are reported in Table I.

All tests were performed by cooling the superconductor with the magnet at 3, 5 mm and very far from the surface in vertical (z) direction, on the centre of the slot in radial direction ($x = 0$) and at 3 mm from the end of the slot in axial direction (y=3 mm). Note that the axial position chosen is not an equilibrium position in axial direction.

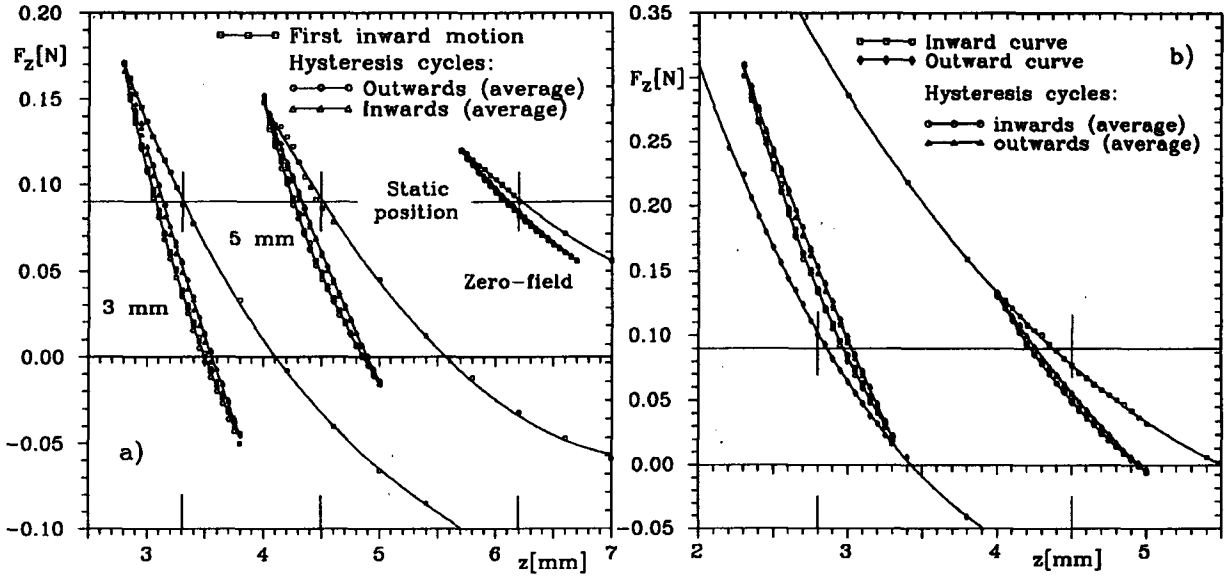

Figure 4. Levitation force as a function of the vertical position of the rotor axis for small movements about the static equilibrium position (a: zero-field cooling and field-cooling at 3 and 5 mm from the surface; b: field-cooling at 5 mm from the surface along the inward and outward branches of the large hysteresis cycle).

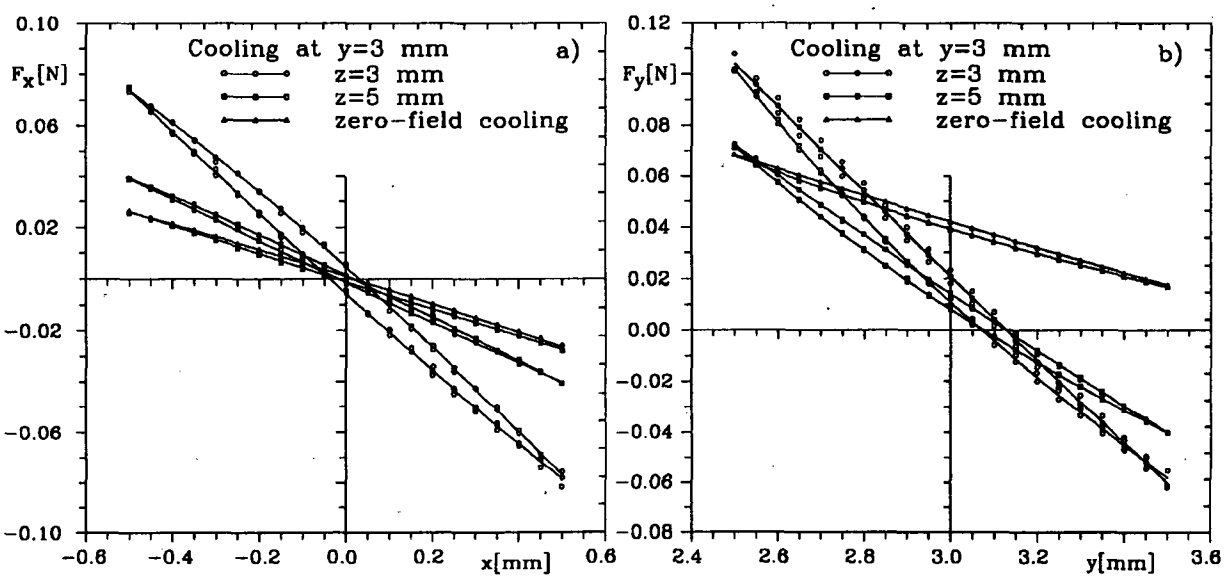

Figure 5. Radial force (a) and axial force (b) as functions of the lateral and axial displacements, when levitating at a distance from the surface of the HTS leading to a force of 0.9 N.

TABLE I - LINEARIZED STIFFNESS AND LOSS FACTOR IN THE VARIOUS DIRECTIONS.

	Stiffness [N/m]			Loss factor		
Cooling at	radial (z)	radial (x)	axial (y)	radial (z)	radial (x)	axial (y)
Zero-field	64.0	53.0	51.1	0.030	0.035	0.053
5 mm	165.0	78.9	111.2	0.065	0.029	0.053
3 mm	216.6	151.3	160.9	0.069	0.060	0.048
Zero-field (upwards)	149.7	--	--	0.054	--	--
5 mm (upwards)	285.9	--	--	0.052	--	--
5 mm (1 magnet)	108.8	--	--	0.044	--	--

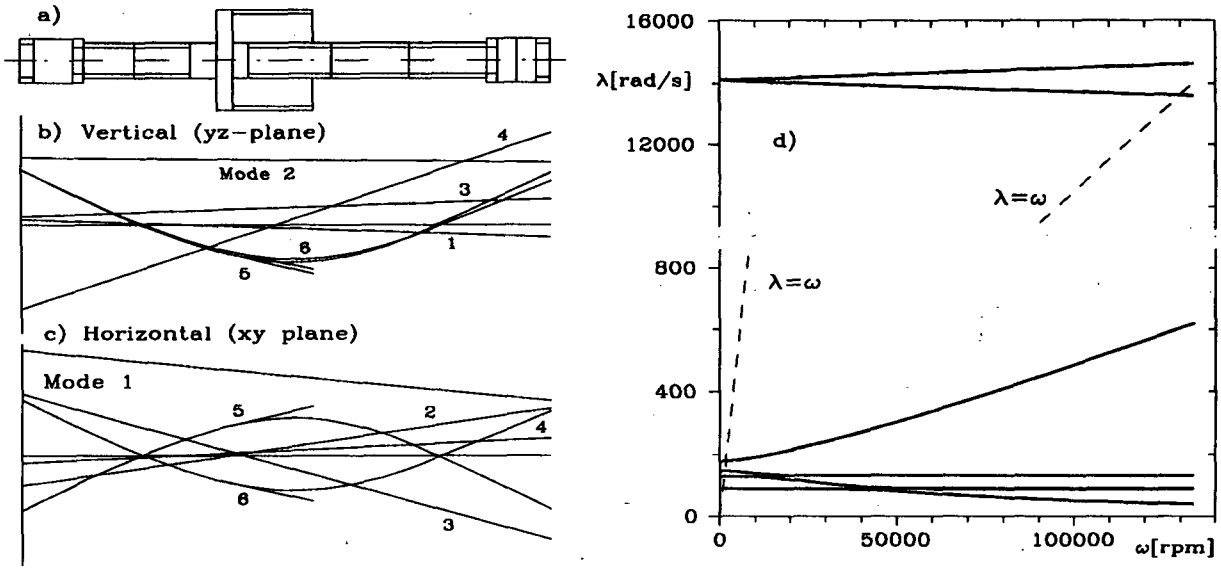

Figure 6. a: FEM model for rotordynamics computations; b and c: mode shapes in the vertical *yz* and horizontal *xy* planes corresponding to the first 6 critical speeds; d: Campbell diagram.

Other tests aimed to obtain values of the cross-components of the stiffness (force in *y* direction due to displacements in *x* direction and so on) were performed. The results showed that this coupling effect exists, partially due to the shape of the slot in the HTS pellet, but, owing to its limited absolute value, they will not be included here and their effect on the dynamic behaviour will be neglected.

DYNAMIC BEHAVIOUR OF THE MACHINE

A mathematical model of the system was built using DYNROT finite element code, developed at Mechanics Department of Politecnico di Torino. Owing to the particular geometry of the magnetic circuit of the motor, no rotor-stator magnetic interaction was taken into account [14]. As the stiffness of the bearing in horizontal and vertical directions are not equal, the approach described in [15] was used to model the unsymmetrical characteristics of the stator.
The values of the first 6 critical speeds for field-cooling at 5 (3) mm are: 832.3 (1177.0), 1222.5 (1421.6), 1393.8 (1785.8), 1694.4 (1992.1), 129860 (129860) and 139970 (139980) rpm. Further critical speeds are encountered above 350000 rpm. The relevant mode shapes are reported in Figure 6, together with the FEM model of the rotor and the Campbell diagram. Note that the presence of the gyroscopic effect (damping has been neglected in this computation) couples *xy* and *yz* planes, and the modes are not vibrations in a plane but are all elliptical motions. The first 4 modes are "rigid body modes" and are very low, while the following ones are "deformation modes" and are well above the working range. Assuming a very coarse balancing quality grade (G40), the eccentricity of the centre of gravity is of 3.18 μm and the static unbalance is $m\varepsilon$=0.0597 g mm. The unbalance response of the damped system obtained for field-cooling at 5 mm with the mentioned value of the unbalance in the centre of gravity of the system has been reported in Figure 7. Note that owing to damping the axes of the elliptical orbits are not exactly parallel to *x* and *z* axes: the values reported in the figure are not exactly the larger and the smaller axes of the orbits. The first 4 critical speeds are easily passed, the maximum values of the amplitudes of the motion being of 0.048, 0.049 and 0.046 mm in vertical direction (at 1222 rpm, second critical speed) respectively at the centre of gravity and at the bearing locations. The maximum values at the same points in horizontal direction are 0.129, 0.153 and 0.09 mm, occurring at 831 rpm. Even lower values would have been obtained, if the angular acceleration with which the first critical speeds are passed were accounted for.

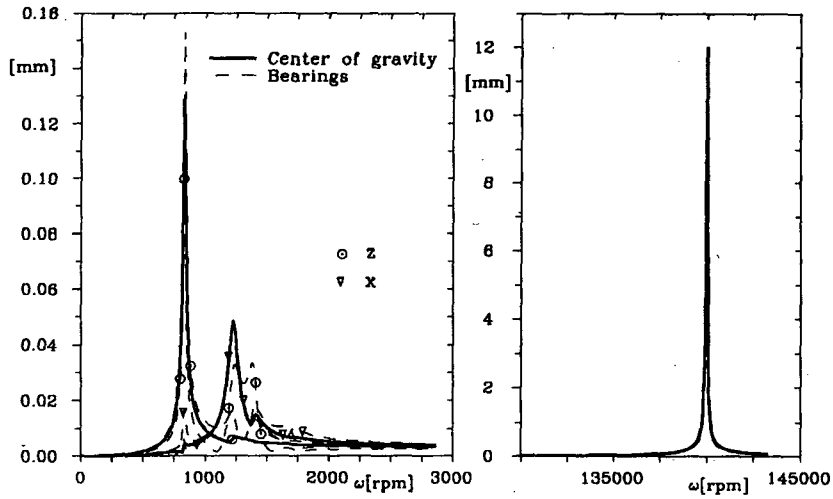

Figure 7. Unbalance response of the rotor computed from the damped model, assuming field-cooling at 5mm and a static unbalance with balancing quality grade G 40.

Note that with the mentioned value of the unbalance, the "deformation" critical speeds cannot be passed: the displacements at 140000 rpm are of about 10 mm in both inflection planes. This is somewhat mitigated by the fact that at this speed the rotor cannot be considered any more as a rigid rotor and a distributed unbalance should be considered instead of an eccentricity of the centre of gravity. In the whole working range the rotor is very well self-centred, with an orbit which is almost circular and has a radius close to the eccentricity (3.18 μm).

These numerical prediction were essentially confirmed experimentally. Several acceleration and deceleration runs were performed, recording the amplitude of the horizontal and vertical displacements of the shaft. The following results were obtained:

- The unbalance of the shaft was not a critical factor; an initial low speed balancing was performed but the actual unbalance condition at each test varied, mainly owing to the ice formations particularly in the zone of the magnets which is cooler and when operating in wet weather. The rotor was very well self-centred at all speeds exceeding 3000 rpm, up the maximum speed reached during the test (105000 rpm).
- At speeds lower than 3000 rpm four resonance peaks are visible. Two of them are mostly linked to vertical motions while other two are mostly horizontal. The peaks at higher speed are well defined, while the other two are more "mixed together" and the various tests gave not very consistent results. They occurred at speeds slightly higher than those computed; e.g., with field-cooling at 5 mm, the two higher measured critical speeds were at 2200 and 2800 rpm against the computed values of about 1400 and 1700 rpm. This seems to indicate that the dynamic stiffness of the superconducting bearings is higher than the measured static stiffness.
- Some magnetic creep was observed. Static tests aimed to verify magnetic creep showed some decrease of the vertical (z-direction) force when the magnet was moved repeatedly in horizontal (x) direction. Similarly, when the motor was repeatedly spun up and down, crossing several times the critical speeds, the equilibrium position was seen to drift downwards, until during a critical speed crossing contact between stator and rotor occurred. The decrease of levitation force seemed to be linked more to the amplitude of the horizontal motion than to time, as sustained running at high speed did not affect the levitation position; this fact could be dominating in assessing balancing tolerances.

EVALUATION OF THE BEARING DRAG

No accurate evaluation of the bearing drag was possible, mainly for the impossibility of operating the motor in vacuum to exclude aerodynamic drag. However, several spin-down tests were performed, recording the spin speed as a function of time (Figure 8a).

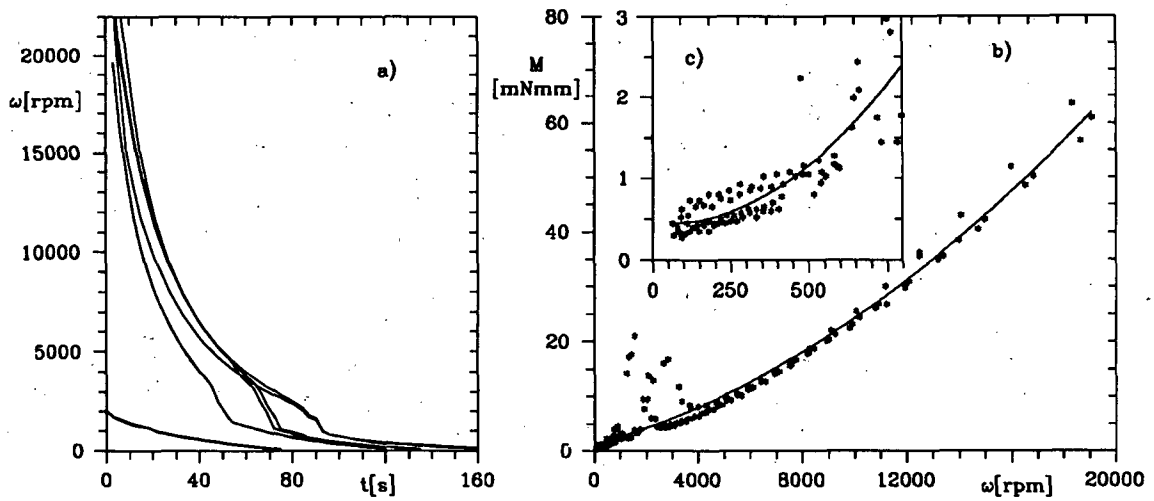

Figure 8. Results of spin-down tests. a: Spin-down curves; b and c: overall drag torque as a function of the speed.

The curves are reported as recorded, with the time measured from the instant in which the driving power was disconnected. The curves show very clearly that during the crossing of the critical speeds the rotor decelerates very quickly, as expected [16]. By differentiating numerically the experimental data, the overall drag torque acting on the rotor could be computed as $M = J\, d\omega/dt$. The results are reported in Figure 8b, for a speed range up to 20000 rpm. Note that, in spite of the fact that the computation of the drag from spin-down tests is always liable to give way to large uncertainties, very consistent results were obtained, at least at speeds not close to the critical speeds.

When crossing the critical speeds the drag torque is much influenced by unbalance, which was not constant; no consistent results could be expected in these conditions. In the graph of Figure 8b a second graph is inset (Figure 8c), related to the speed range from 0 to 800 rpm. In this case the amplitude of the motion is again quite affected by unbalance and the results are more scattered, but the trend is clear. In both graphs the points are interpolated by a least-square cubic polynomials.

The drag torque measured, which is of the order of some tens of mN mm, includes mainly 3 forms of drag: aerodynamic drag, drag due to nonrotating damping in whirling conditions and magnetic bearing drag. It was found impossible to extract the third component from the experimental results, due to the uncertainties of the evaluation of the aerodynamic drag torque, of nonrotating damping and unbalance. However, the overall drag torque measured was very small and it supplies an order of magnitude for the maximum drag to be expected from the bearing system.

CONCLUSIONS

Passive high speed superconducting magnetic bearings made by melt-textured Y-123 may turn out to be one of near-term applications of HTS. To evaluate their potential use, prototypes of HTS $YBa_2Cu_3O_{7-x}$ bearings have been manufactured and used to suspend the rotor of an asynchronous motor operating up to 120000 rpm. For a better understanding of the magnet/superconductor interaction, the characterization of the bearings, in terms of magnetic force vs. rotor height, magnetic stiffness and rotational decay, was performed.

The static tests showed that the bearings exhibit a strong hysteretic behaviour, both for what the behaviour "in the large" and that "in the small" are concerned. The levitation force and the stiffness of the bearing was found to be much sensitive to the relative position of the magnet and the superconductor during cooling. The behaviour in the small can be linearized, allowing to model the support using the "hysteretic damping" model: both the stiffness and the damping

factor in vertical and horizontal directions have been measured with different cooling positions. Although no detailed measurement of the cross-coupling terms was performed, some tests did show that they are not vanishingly small.
The rotor was spun up to 105000 rpm, the maximum speed allowed by the frequency converter available. The rotation tests showed that the dynamic behaviour of the rotor is close to that computed using the methods of linear rotordynamics, and particularly the very ample tolerance to unbalance which was predicted was experimentally checked. The values of the critical speeds measured were higher than those computed, which indicates that the dynamic stiffness of the bearings is higher than the static stiffness.
The spin-down tests allowed to compute the overall torque acting on the rotor, which was found to be very small. No attempt to separate the bearing and aerodynamic drag was performed.
Some magnetic creep was evidenced when the rotor worked for long times with ample whirling motions. This aspect, which could be a severe limiting factor in the application of superconducting bearings, particularly for what the sensitivity of the suspension to unbalance forces is concerned, is now the subject of further investigations on a larger bearing prototype.

REFERENCES

1. Ricca, A.. 1987. "Una Nuova Frontiera: i Materiali Ceramici Superconduttori", Energia e Materie Prime,, X(57):55-62.

2. Murakami, M., T. Oyama, H. Fujimoto, S. Gotoh, K. Yamaguchi, Y. Shiohara, N. Koshizuaka, and S. Tanaka. 1991. "Melt Processing of Bulk High Tc Superconductors and Their Application", IEEE Transactions on Magnetics,, 27(2):1479-1486.

3. Murakami, M., T. Oyama, H. Fujimoto, T. Taguchi, S. Gotoh, Y. Shiohara, N. Koshizuka, and S. Tanaka. 1990. "Large Levitation Force due to Flux Pinning in YBaCuO Superconductors Fabricated by Melt-Powder-Melt-Growth Process", Japanese Journal of Applied Physics,, 29(11):1991-1994.

4. Moon, F.C.. 1990. "Magnetic Forces in High-Tc Superconducting Bearings", Applied Electromagnetics in Materials,, 1:29-35.

5. Hull, J.R., T.M. Mulcahy, L. Lynds, B.R. Weinberger, F.C. Moon, and P.Z. Chang. August 1990. "Phenomenology of Forces Acting Between Magnets and Superconductors", Proc. 25th I.E.C.E.C., Reno, NV, USA.

6. Moon, F.C., K.C. Weng, and P.Z. Chang. 1989. "Dynamic Magnetic Forces in Superconducting Ceramics", Juornal of Applied Physics,, 66(11):5643-5645.

7. Yotsuya, T., M. Shibayama, and R. Takahata. 1991. "Characterization of High-Temperature Superconducting Bearing", in Proc. CEC'91, Huntsville, AL, USA, BE4.

8. Moon, F.C., M.M. Yanoviak, and R. Ware. 1988. "Hysteretic Levitation Forces in Superconducting Ceramics", Appl. Phys. Lett.,, 52(18):1534-1536.

9. Weinberger, B.R., L. Lynds, J.R. Hull, and U. Balachandran. 1991. "Low Friction in High Temperature Superconductor Bearings", Appl. Phys. Lett.,,59(9):1132-1134.

10. Moon, F.C., and P.Z. Chang. 1990. "High-Speed Rotation of Magnets on High Tc Superconducting Bearings", Appl. Phys. Lett.,, 56(4):397-399.

11. Moon, F.C., and J.R. Hull. August 1990. "Materials Research Issues in Superconducting Levitation and Suspension as Applied to Magnetic Bearings", Proc. 25th I.E.C.E.C., Reno, NV, USA.

12. Jayawant, B.V.. 1982. "Electromagnetic Suspension and Levitation",, IEE Proc.,, 129(8):549-581.

13. Bean, C.P.. 1964. "Magnetization of High-Field Superconductors", Reviews of Modern Physics,, 36(1):31-39.

14. Widmer, J., G. Genta, P. Von Burgh, and H. Asper. August 1988. "Prediction of the Dynamic Behaviour of a Flywheel-Rotor System by FE Method", Proc. 23rd I.E.C.E.C., Denver, Colorado, USA, 2:97-104.

15. Genta, G.. 1988. "Whirling of Unsymmetrical Rotors, a Finite Element Approach Based on Complex Co-ordinates", Journal of Sound and Vibration,, 124(1):27-53.

16. Genta, G. Vibration of Structures and Machines, Springer, New York, USA, to be published.

ACKNOWLEDGEMENTS

The present work was partially supported by the National Agency of Electricity (ENEL), by the National Research Council of Italy under the Progetto Finalizzato "Superconductive and Cryogenics Technologies" and by Italian Ministry of University and Scientific Research under the 60% and 40% research grants.